EXAMINATION OF SPHERICAL ANTENNA FAR-FIELD SCATTERING SUPPRESSION THROUGH ELECTROMAGNETIC SIMULATION

Zhengrong Tian[1], Stuart F Gregson[2]

[1]National Physical Laboratory, Teddington, UK
[2]Queen Mary University of London, London, UK
**Zhengrong.Tian@npl.co.uk*

Keywords: ANTENNA, SPHERICAL ANTENNA MEASUREMENT, ELECTROMAGNETIC SIMULATION, SCATTERING SUPPRESSION

Abstract

For any indoor antenna test range (planar/cylindrical/spherical/compact), room scattering is one of the most significant terms within the overall uncertainty budget, especially when the range is pushed to operate outside its optimal working frequency range, either lower or higher than its designed frequency range. A frequency domain mode filtering based measurement technique has been used to reduce the range scattering in the past decade. Although this technique has been extensively examined and validated through measurements, comparatively little validation has been reported using full-wave three-dimensional computational electromagnetic (EM) simulation because of the huge computational effort required. Built upon the successful, recent, development of an EM model for cylindrical mode based far-field antenna scattering suppression, that study is extended to consider the more complicated case of the spherical far-field range. For the first time, an EM model of the spherical far-field measurement was constructed and used to verify this measurement and post-processing technique. The EM modelling technique is detailed, and initial results are presented which show good agreement between the "true" far-field and the perturbed far-field with scattering suppression processing having been applied. The criterion of how to select the transformation centre point for optimal scattering suppression is examined and best practice proposed.

1 Introduction

Room scattering is one of the most significant error sources that affects the accuracy of antenna measurement carried out indoors [1]. A frequency domain mode filtering based scattering suppression technique has been successfully used to reduce the range scattering in the past decade [2-8]. Although the technique has been validated and examined through extensive measurements, there is a need to further examine this technique through EM simulation in order to quantify the level of effectiveness of the scattering suppression and for determining the optimal application of this technique. The idea is to construct a digital replica of the antenna measurement in the test range by means of EM modelling. The advantage of using EM simulation is that the "measurement" can be carried out in a controlled environment numerically, and the absolute "truth" model, *i.e.*, the simulated antenna pattern can be used as the benchmark to enable precise and quantified examination, whereas it has not been possible to achieve this simply through measurement due to the lack of a definitive "truth" model. This idea has been successfully tested through our previous work on an EM model for cylindrical mode based far-field antenna scattering suppression [9]. In this paper, the EM model for much more complicated spherical antenna measuring over the full 4π steradian sphere has been constructed and simulated.

In the following section, an overview of the mode filtering-based scattering suppression technique for antenna measurement in a spherical test range is first described, followed by the details of the construction method of the EM model. The relationship between the spherical wave mode coefficients (SMCs) of the antenna and the measurement rotation centre is carefully examined, which leads to the recommendation of how to select the transformation center for optimal scattering suppression. Finally, the simulated results of spherical far-field before and after scattering suppression are compared and presented. The paper concludes with a summary and the planned future work.

2 Overview of the Technique

The scattering suppression technique is general and can be applied to any antenna range, *i.e.*, planar, cylindrical, spherical, or compact. The key feature of the technique is to perform the pattern acquisition with the antenna under test (AUT) positioned with an offset from the measurement rotation center, unlike the conventional measurement in which the AUT is carefully placed at the rotation centre. The details of the scattering suppression technique can be found in the open literature [2]. This paper focusses the study for the spherical antenna test case and Fig. 1 summarises the steps that have been taken for spherical scattering suppression as treated in this paper.

Step 1. Acquire spherical far-field amplitude and phase pattern with the AUT offset from the origin of the measurement coordinate system. The amount of offset should be large enough in order for the higher order modes to be identified. The acquisition increment Δθ is determined by:

$$\Delta\theta = \frac{180°}{kr_0 + 10} \qquad (1)$$

Where k is the wave factor: $k=2\pi/\lambda$ and r_0 is the maximum radial extent (MRE) of the AUT, which is determined by the size of the AUT and also the relative position of the AUT with respect to the origin of the measurement coordinate system.

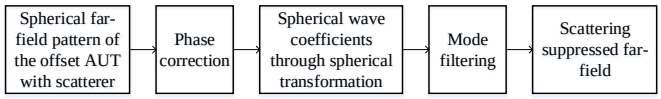

Fig. 1 Flow chart: spherical scattering suppression data process

Step 2. Apply phase correction to translate the measured antenna pattern back to the origin of the measurement coordinate system. Equation (1) shows the phase correction equation when the AUT is offset along the Z axis only.

$$\text{Phase Correction} = 2\pi Z_{offset}\frac{\cos(\theta)}{\lambda} \qquad (1)$$

Step 3. Compute the SMCs through spherical transformation.

Step 4. Apply a mode filter to the SMCs obtained in step 3 to remove the higher order mode associated with the scatterer and only keep the fundamental mode that is associated with the AUT.

Step 5. Compute the far-field using the mode filtered SMCs obtained in step 4 to calculate the far-field with reduced scattering.

3 The EM Modelling

The EM model (Fig. 2) consists of a WR75 standard gain horn as the AUT, which has an aperture size of 94 mm × 67 mm and length of 200 mm. The AUT was placed with its aperture behind the rotation centre (0,0,0) by 360 mm. The AUT port is assumed to be a WR75 waveguide port. A metallic plate with size of 200 mm × 200 mm and with its centre located at (-2000, 0, 3000) (unit in mm) is used as a scattering object to perturb the measurement. The red dot at the left bottom of Fig. 2 is the conceptual far-field point at θ = 0° and φ =0°.

It can be seen that due to the presence of the scatterer, the problem becomes an electrically large problem. CST integral equation solver was used for the simulation as it is a specialised solver which is well suited to the treatment of electrically large structures which comprise principally metallic constituent parts.

When the AUT is measured in a spherical antenna measurement configuration, the AUT steps in θ with increment of Δ θ and scans in φ with increment of Δ φ around the rotation centre. This is illustrated in Fig. 3 (a). When the AUT is rotated to an acquisition point of (θ_i, φ_i), in most cases, the AUT waveguide port is not aligned to the Cartesian coordinate system associated with the problem space. Unfortunately, this is not permitted by the EM simulation software. To overcome this limitation, the model is constructed by keeping the AUT fixed, but instead rotating the metal plate as well as the conceptual far-field point. One simulation file is generated per combination of (θ_i, φ_i). This process is fully automated by means of a dedicated macro. The far-field of each model at (θ_i, φ_i) is simulated. A second macro was developed to extract the far-field at the specific far-field point (θ_i, φ_i) from each corresponding model and then subsequently combine the far-field at each (θ_i, φ_i) to form the complete simulated perturbed spherical far-field pattern measurement of the AUT.

The far-field of the AUT itself, *i.e.* without the scatterer, is also simulated conventionally and this is used as the bench-mark for the examination.

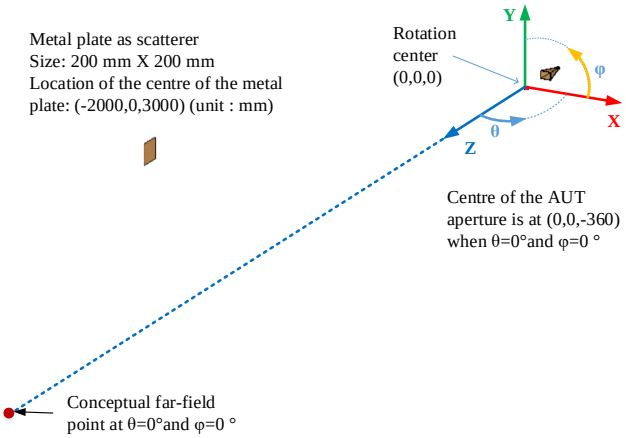

Fig. 2 Illustration of an EM model for spherical far-field antenna measurement using scattering suppression technique

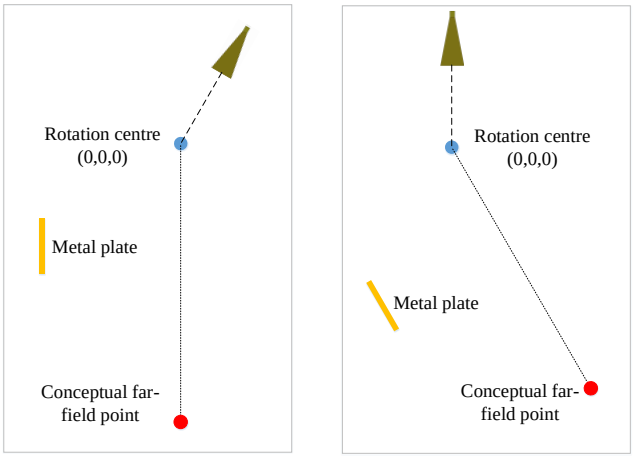

(a) Rotation of the AUT

(b) Rotation of the metal plate and the conceptual far-field point

Fig. 3 EM model at (θ_i, φ_i): (a) Rotation of the AUT; (b) Rotation of the metal plate and the conceptual far-field point.

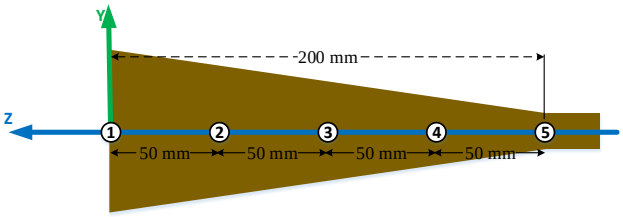

Fig. 4 Illustration of the position of various rotation centres

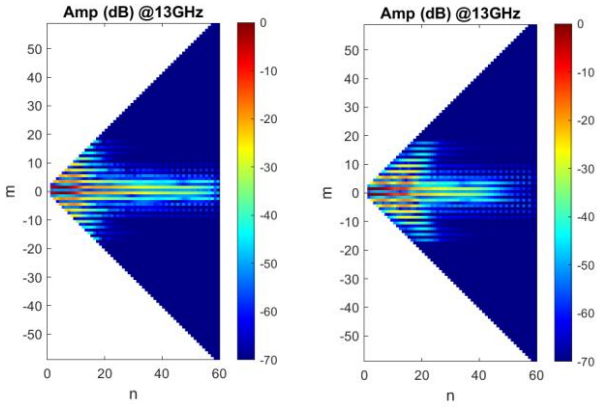

(a) Position 1

(b) Position 2

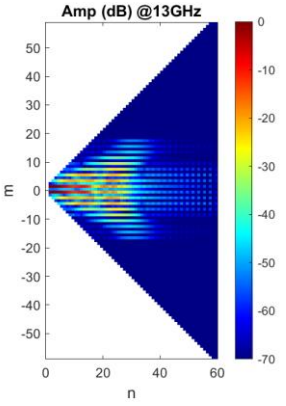

(c) Position 3

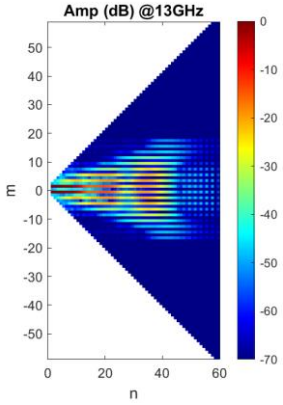

(d) Position 4

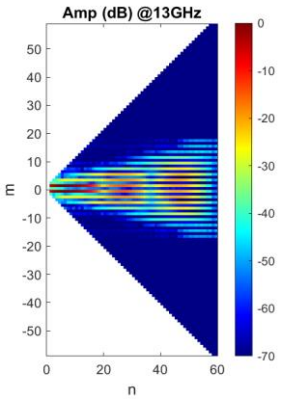

(e) Position 5

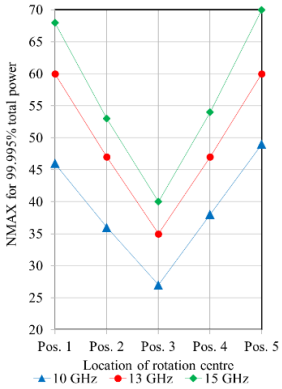

(f) N_{MAX} required for 99.9995% Power

Fig. 5 (a) to (e) Amplitude of SMCs with rotation center located at different positions. (f) Number of spherical wave modes for containing 99.9995% of the total radiated power.

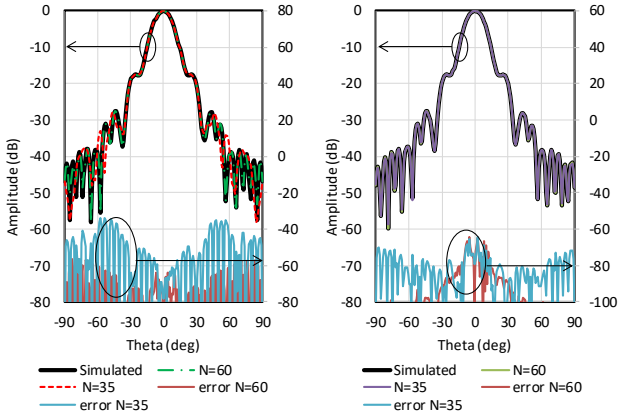

(a) rotation centre at aperture

(b) rotation centre at the middle of the horn

Fig. 6 Pattern comparison when different number of spherical wave modes are used: (a) rotation centre at the AUT aperture; (b) rotation centre at the mid length of the AUT.

It is worth noting that the same phase reference for each model at different (θ_i, φ_i) must be maintained, and this can be achieved by setting the same phase origin when exporting the far-field from the simulation results.

4 Simulation Results

4.1 Transformation Centre for Phase Correction

As shown in Fig. 1, once the perturbed far-field is obtained, the next step is to apply phase correction using Equation (1). The question is what value should be used for Z_{offset}. The purpose of phase correction is to conceptually translate the AUT back to the measurement origin, *i.e.*, the rotation centre. However, since the AUT has a certain length, it is not clear which part of the AUT should be brought back to the rotation centre.

The essence of the scattering suppression is to be able to separate the fundamental modes belong to the AUT and the

higher order modes created by the scatterer. So ideally the AUT should be positioned in such a way that only a minimal number of spherical wave modes is necessary for representing the AUT. With the help of EM software, we are able to examine the relationship between the number of spherical wave modes required for representing the AUT (referred to as N_{MAX}) and the location of the rotation centre relative to the AUT. To achieve this, the far-field of the AUT without the metal plate was simulated with the rotation centre located at different places evenly distributed along the length of the AUT as shown in Fig. 4.

For each case, the far-field was simulated and the corresponding complex SMCs were calculated [10]. The amplitude of the SMCs at 13 GHz are plotted in Fig. 5 (a) to (e). It can be seen here that the energy distribution in the spherical wave modes varies with the location of the rotation centre. Fig. 5 (f) shows the N_{MAX} required for containing 99.9995% of the total power when the rotation centre is located at different places for frequency at 10 GHz, 13 GHz and 15 GHz. It can be seen for all three frequencies simulated, the N_{MAX} is at a minimum when the rotation centre is placed at the mid length of the AUT. This feature is also observed through measurements carried out in the spherical test range.

Fig. 6 further demonstrates the effect when different numbers of spherical wave modes are used for representing the AUT. Fig. 6 (a) shows that when the rotation centre is at the AUT aperture, if N_{MAX} of 35 is used, the truncation error due to the fact that not enough modes have been included can be as high as -34 dB, but the truncation error can be reduced to -56 dB if N_{MAX}=60. When the rotation centre is located at the mid length of the AUT (Fig. 6 (b)), the truncation error is -64 dB whether N_{MAX}=60 or N_{MAX}=35. This investigation suggests that for phase correction, the AUT should be brought back so that the rotation center is located at the mid length of the AUT. Fig. 7 presents the surface current contour plot of the AUT which shows quite a lot of currents flowing on the flaring metal waveguide. The smallest sphere that contains the majority of the current sources is when the rotation centre is placed half way along the length of the horn.

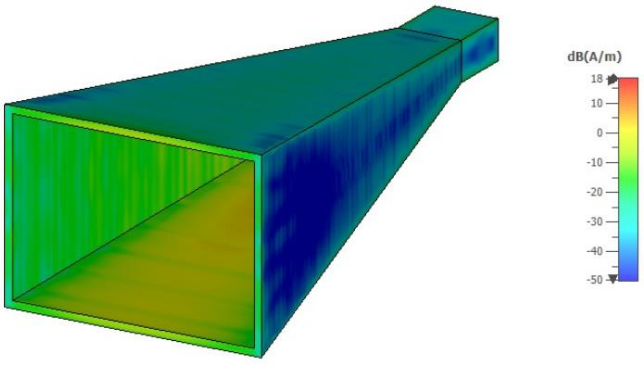

Fig. 7 Surface current contour plot.

4.2 Results of Scattering Simulation

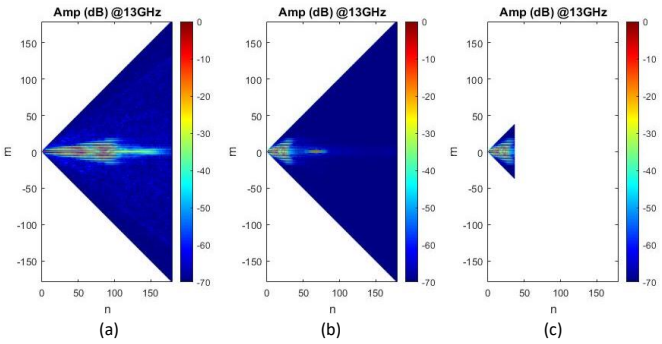

Fig. 8 Amplitude of the spherical wave coefficients at 13 GHz (a) before phase correction; (b) after phase correction; (c) after mode filtering

After applying the phase correction to the simulated perturbed far-field, the SMCs were calculated using the standard spherical transformation whereupon a low-pass mode filter was applied. Fig. 8 (a) shows the amplitude of the SMCs of the simulated perturbed field. There is clear presence of the higher order mode. Fig. 8 (b) shows the amplitude of the SMCs after the phase correction has been applied, from which the separation between higher order modes and fundamental modes can be observed. And finally, Fig. 8 (c) shows the amplitude of the SMCs having mode filtering applied, and this is the SMCs used for calculating the far-field pattern, now with reduced scattering artefacts.

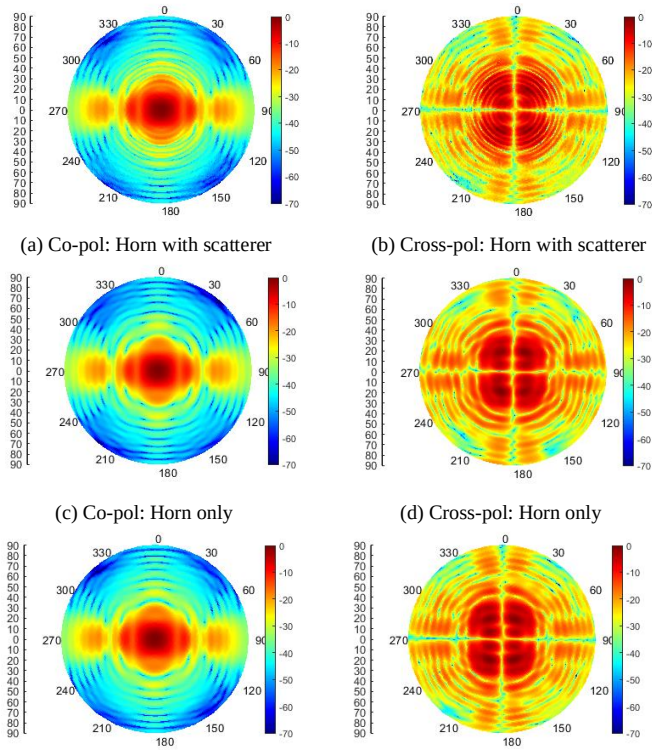

(a) Co-pol: Horn with scatterer

(b) Cross-pol: Horn with scatterer

(c) Co-pol: Horn only

(d) Cross-pol: Horn only

(e) Co-pol: Mode filtered

(f) Cross-pol: Mode filtered

Fig. 9 Comparison of the co-pol and cross-pol of the far-field pattern: (a) and (b) horn with scatterer; (c) and (d) horn only; (e) and (f) mode filtered.

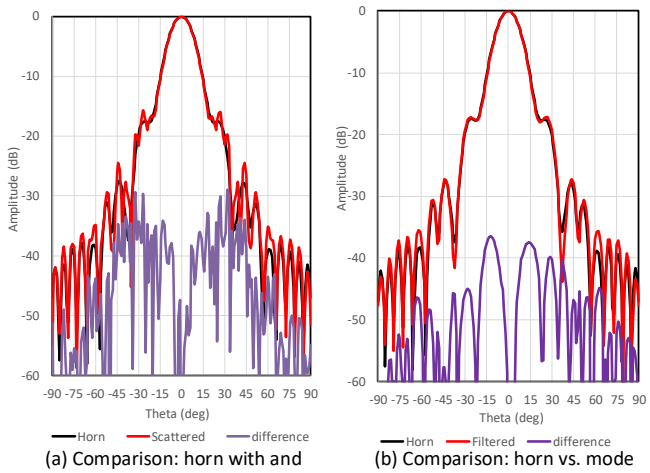

(a) Comparison: horn with and without scatterer

(b) Comparison: horn vs. mode filtered

Fig. 10 Comparison of boresight pattern cut: horn only, with scatterer and mode filtered.

Fig. 9 compares the co- and cross-pol of the AUT itself, AUT with scatterer and again with the mode filter applied. Fig. 9 (a) and (b) present the simulated co- and cross-pol far-field pattern with the scatterer introduced, there is clear ripple presence. Fig. 9 (c) and (d) show the simulated far-filed pattern of the horn itself, without the presence of any scatterer, and this is served as a benchmark for the comparison. The far-field pattern with mode filtering scattering suppression data post process applied are shown in Fig. 9 (e) and (f), from which it can be observed that the ripples have been effectively removed.

Fig. 10 plots the boresight pattern cut for more closer examination. The red curve in Fig. 10 (a) is the boresight pattern cut of the simulated horn with scatterer, where strong ripples appear around $\theta = \pm 30°$. Comparing with the simulated pattern of the horn itself (the black curve), the error due to the scattering caused by the metal plate is about -30 dB at $\theta = \pm 30°$. Fig. 10 (b) shows the boresight pattern cut when the scattering suppression data post processing has been applied, and it is clear that the ripple at $\theta = \pm 30°$ has been effectively removed and the error due to the scattering has been reduced to about -45 dB.

5 Conclusion

An EM model which serves as a digital replica of a spherical far-field antenna measurement has been constructed and validated. A 3D far-field pattern dataset was obtained through EM simulation with the AUT offset from the rotation centre and a metal plate introduced as a scatterer. This dataset was valuable which enables quantified examination of the effectiveness of the mode filtering technique on scattering reduction, yielding a particularly encouraging degree of improvement in the cross-polar pattern, and also enables optimisation of the scattering suppression data post process. Initial examination on pyramidal type horn suggests improved scattering suppression can be obtained by mathematically move the mid length of the horn to the measurement rotation centre. Future work is to expand this investigation to other types of antenna and examine the relationship between the number of modes required for representing the AUT and the location of the measurement rotation centre with the intention to provide best practice on application of the mode filtering based scattering suppression technique for optimal scattering reduction effect.

6 Acknowledgements

The authors gratefully acknowledge the funding support provided by the UK National Measurement System and the Department for Business, Energy and Industrial Strategy (BEIS) that enabled the work that this paper presents.

7 References

[1] A.C. Newell, “Error Analysis Techniques for Planar Near-field Measurements”, IEEE Transactions on Antennas and Propagation, vol. AP-36, pp. 754-768, June 1988.

[2] C.G. Parini, S.F. Gregson, J. McCormick, D. Janse van Rensburg, “Theory and Practice of Modern Antenna Range Measurements”, IET Press, 2014, ISBN 978-1-84919-560-7.

[3] G.E. Hindman, A.C. Newell, “Reflection Suppression in a large spherical near-field range”, AMTA 27th Annual Meeting & Symposium, Newport, RI, October 2005.

[4] G.E. Hindman, A.C. Newell, “Reflection Suppression To Improve Anechoic Chamber Performance”, AMTA Europe 2006, Munch, Germany, March 2006.

[5] S.F. Gregson, A.C. Newell, G.E. Hindman, “Reflection Suppression In Cylindrical Near-Field Antenna Measurement Systems – Cylindrical MARS”, AMTA 31st Annual Meeting & Symposium, Salt Lake City, UT, November 2009.

[6] S.F. Gregson, A.C. Newell, G.E. Hindman, “Reflection Suppression in Cylindrical Near-Field Measurements of Electrically Small Antennas”, Loughborough Antennas & Propagation Conference, November, 2009.

[7] S.F. Gregson, A.C. Newell, G.E. Hindman, M.J. Carey, “Extension of the Mathematical Absorber Reflection Suppression Technique to the Planar Near-field Geometry”, AMTA, Atlanta, GA, October, 2010.

[8] S.F. Gregson, A.C. Newell, G.E. Hindman, P. Pelland, “Range Multipath Reduction in Plane-Polar Near-field Antenna Measurements”, AMTA, Seattle, October 2012.

[9] Z. Tian, S.F. Gregson, “Examination of the Effectiveness of Mode Orthogonalisation and Filtering for Scattering Suppression in Antenna Measurements Through Computational Electromagnetic Simulation”, EuCAP, Krakow, 2019.

[10] A. Frandsen, F. Jensen and f. Larsen, “Spherical Near-Field Transformation Program with Probe Correction, Manual for computer Program SNIFTD”, TICRA A/S Engineering Consultants, November 1985.